

Energy and pitch angle-resolved measurements of escaping helically trapped energetic ions at the small major radius side of the compact helical system

M. Isobe^{a)}

National Institute for Fusion Science, 322-6 Oroshi-cho, Toki-shi 509-5292 Japan

D. S. Darrow

Princeton Plasma Physics Laboratory, Princeton, New Jersey 08543

J. Kotani

Nagoya University, Nagoya-shi 464-8602 Japan

A. Shimizu, C. Suzuki, Y. Yoshimura, T. Minami, C. Takahashi, K. Nagaoka, S. Nishimura, K. Toi, K. Matsuoka, S. Okamura, and the CHS group

National Institute for Fusion Science, 322-6 Oroshi-cho, Toki-shi 509-5292 Japan

(Presented on 9 July 2002)

We have developed and installed a new, second escaping fast ion probe for the small major radius side of the compact helical system. This is a Tokamak Fusion Test Reactor type scintillator-based probe and is intended to detect unconfined helically trapped fast ions whose orbits largely deviate from magnetic flux surfaces. We observed a localized light spot on the scintillator screen in neutral beam-heated discharges and it was confirmed to be a true fast ion signal. The analysis suggests that the probe detects partially thermalized, pitch angle scattered beam ions. © 2003 American Institute of Physics. [DOI: 10.1063/1.1538330]

I. INTRODUCTION

Escaping fast ion measurements have been carried out in the compact helical system (CHS) heliotron/torsatron by the use of a scintillator-based probe. We installed the first escaping fast ion probe for the large major radius R side in 1997.¹⁻⁴ This probe has detected lost co-going barely transit beam ions, which deviate substantially from magnetic flux surfaces to the outboard side, and transitional ions. It has so far provided valuable information for not only losses of neutral beam (NB) ions via neoclassical transport processes but also fishbone type magnetohydrodynamics (MHD) induced losses.^{5,6} In order to measure energetic ions having different types of orbits and to understand NB ion behavior in further detail, we have designed and installed a new, second escaping fast ion probe for small R side of the CHS. This new probe is intended to detect unconfined helically trapped fast ions whose orbits deviate significantly from magnetic flux surfaces to the inboard side. In this article, we describe an idea of the new escaping fast ion probe for the small R side of the CHS and initial experimental results.

II. EXPERIMENTAL SETUP

A. CHS and perspective for trapped ion orbits

The compact helical system is a heliotron/torsatron type device with device major radius R of 1 m and an average minor radius of about 0.2 m.⁷ The toroidal and poloidal period numbers are $N=8$ and $l=2$, respectively. The toroidal magnetic field B_t can be increased up to 2 T. B_t is typically

directed to be counterclockwise as seen from the above. The target plasma is initiated by electron cyclotron resonance heating (ECRH). Two NB injectors (NB 1:38 keV/0.8 MW; NB 2:30 keV/0.8 MW) are installed in the same direction. Both NBs are usually coinjected.

One of major concerns in the CHS experiment is the confinement property of energetic ions, especially helically trapped ions, because of rippled magnetic field. In order to make this argument clear, we show Mod- B_{\min} contours, i.e., traces of the bottom of the helical ripple well for the standard configuration ($R_{ax}=0.921$ m) of the CHS in Fig. 1.⁸ It can be seen that Mod- B_{\min} contours are not well aligned with the magnetic flux surfaces. Figure 1 suggests that a helically trapped ion orbit deviates from the magnetic flux surface to

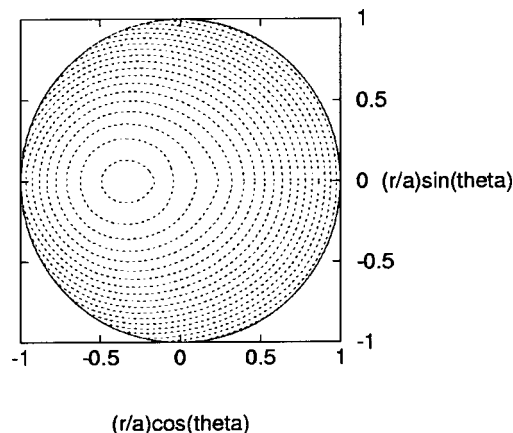


FIG. 1. Mod- B_{\min} contours of the vacuum magnetic field of the CHS ($R_{ax}=0.921$ m).

^{a)}Electronic mail: isobe@nifs.ac.jp

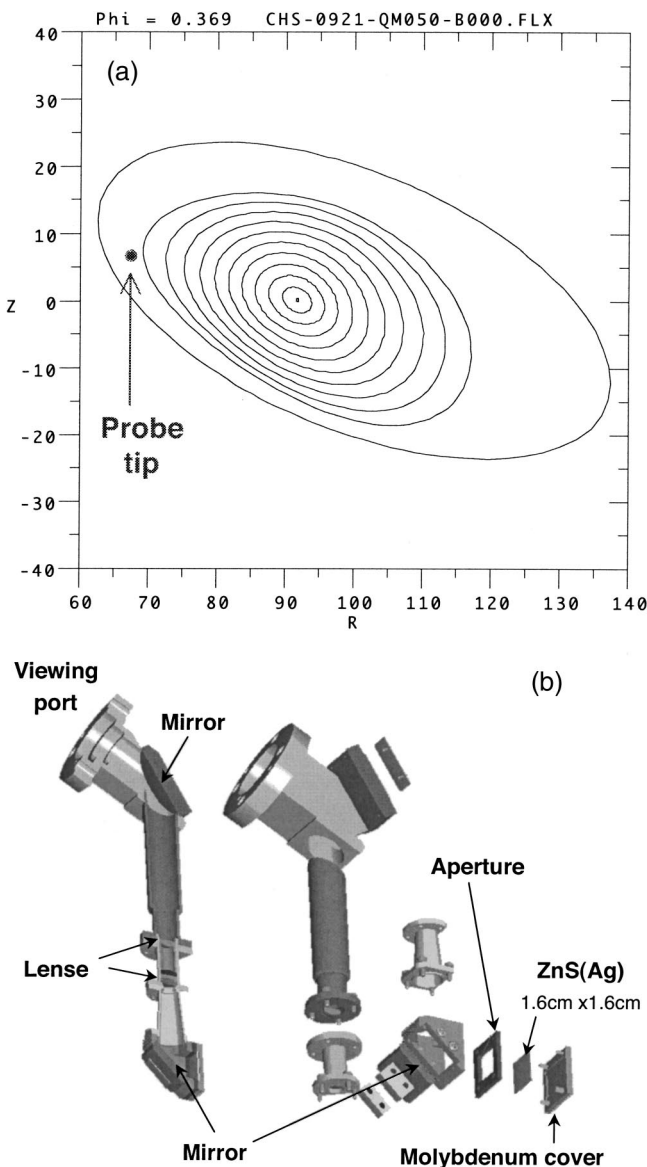


FIG. 2. (a) Poloidal cross section of the vacuum vessel and plasma where the lost fast ion probe is installed. (b) Schematic drawing of the outside appearance and structure of the probe.

the inboard side, and will cross the outermost flux surface and then intersect the vacuum vessel wall at the small R side because these ions tend to move along the bottom of the helical ripple well.

B. Lost fast ion probe at small R side

After we chose a diagnostic port suitable for our purpose and a probe position where ions are expected to be lost, the probe design was carefully carried out by the use of a three-dimensional computer aided design (CAD) software because the plasma touches the inboard vacuum vessel wall at a vertically elongated cross section, and then the space available for the probe installation is very limited at the small R side of the CHS. The poloidal cross section of the vacuum vessel and the CHS plasma where the probe is installed is shown in Fig. 2(a). The probe tip is at $R=0.68$ m and $z=+0.06$ m from the equatorial plane, and is 1–2 cm away from the plasma boundary. We choose a smaller ZnS(Ag) scintillator

smear on a quartz substrate of $1.6\text{ cm} \times 1.6\text{ cm}$ than that ($2.5\text{ cm} \times 2.5\text{ cm}$) of first probe because in addition to the limited space, somewhat slowed down, pitch angle scattered beam ions are expected to be detected. The outside appearance and structure of the new probe are schematically illustrated in Fig. 2(b). The idea of this probe basically originates in the fast ion probe used for a Tokamak Fusion Test Reactor (TFTR).^{9,10} The scintillator plate is mounted inside a molybdenum box and is set with its back against the plasma. The probe contains two apertures, which disperse the beam ions according to gyroradius and pitch angle onto the scintillator. The vector perpendicular to the plane of the apertures is directed to be upward, i.e., in the $+z$ direction. The first aperture is 0.8 mm high and 1.0 mm wide and the second aperture is 0.8 mm high and 8.0 mm wide. Ions with larger gyroradii hit the scintillator surface farther from the aperture than those with smaller gyroradii. Concerning the pitch angle, ion strike points are dispersed across the line passing through the center of two apertures according to their pitch angle. The two-dimensional (2D) scintillation image due to fast ion impacts is guided to a viewing window mounted on a diagnostic port by the use of a glass lens and metal mirror system inside the stainless steel probe shaft and then transferred to an image intensified a charged-coupled-device (CCD) camera (Princeton Instruments Co., model PENTAMAX512) via a quartz optical image fiber (Mitsubishi Densen Co., model SBD15-A1010). The image data are typically accumulated during 50 ms and stored in a personal computer based on the Windows NT system. In order to record a time trace of scintillation light intensity with fast sampling frequency, the 2D scintillation image is split by the use of a pellicle beam splitter and is measured by a photomultiplier (Hamamatsu Co. model H5784).

III. OBSERVATION OF LOST HELICALLY TRAPPED FAST IONS

A localized bright spot on the scintillator screen due to fast ion impact has been observed in the neutral beam-heated plasma of the CHS. Figure 3 indicates a typical scintillation light spot appeared on the screen in $B_t=1.76$ T and $R_{ax}=0.921$ m. The local magnetic field strength at the probe tip position is 1.56 T in this case. The grid of the pitch angle versus gyroradius centroid is computed by taking account of the local magnetic field vector at the probe position and geometrical information such as the direction of the aperture and scintillator plate and their size. The analysis indicates that the gyroradius and pitch angle [$\chi=\arcsin(v_{\parallel}/v)$] of escaping ions we detect is 0.5–1.5 cm and 60° – 75° , respectively. The energy of detected lost fast ions is roughly 5–20 keV. We changed the injection angle of the NB from a tangency radius of 0.87 m, which is parallel and the best angle in the plasma heating, to 0.49 m, to check whether the position of the light spot on the scintillator screen changes. No significant difference in the scintillation image was observed between parallel and perpendicular NB injection. The possible reason for this observation might be that the loss cone structure is the same irrespective of beam injection angle. In order to interpret this observation, a careful analysis will be carried

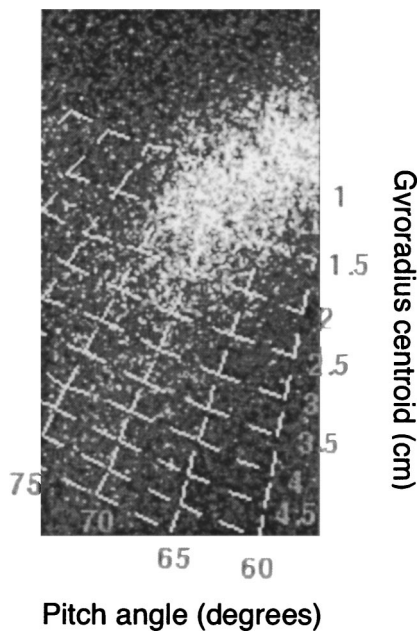


FIG. 3. Typical light spot appearing on the scintillator screen due to fast ion impact. NB is tangentially coinjected. B_t and R_{ax} were 1.76 T and 0.921 m.

out by the global calculation for beam ions including collision effects. The full gyromotion following orbit calculation indicates that fast ions making a localized bright spot have unconfined helically trapped and transitional orbits. Orbits of lost trapped fast ions reaching the probe are shown in Fig. 4. Because the NB is tangentially injected in the CHS, these are supposed to be pitch angle scattered, partially thermalized ions during their deceleration process. A typical temporal evolution of line averaged electron density n_e , $H\alpha$ light intensity, and scintillation light intensity, i.e., fast ion loss rate to probe is shown in Fig. 5. After the NB is injected, the ZnS(Ag) begins to emit the scintillation light and its intensity gradually increases in time. The fast ion loss rate to probe is enhanced further after the second NB is injected. The point

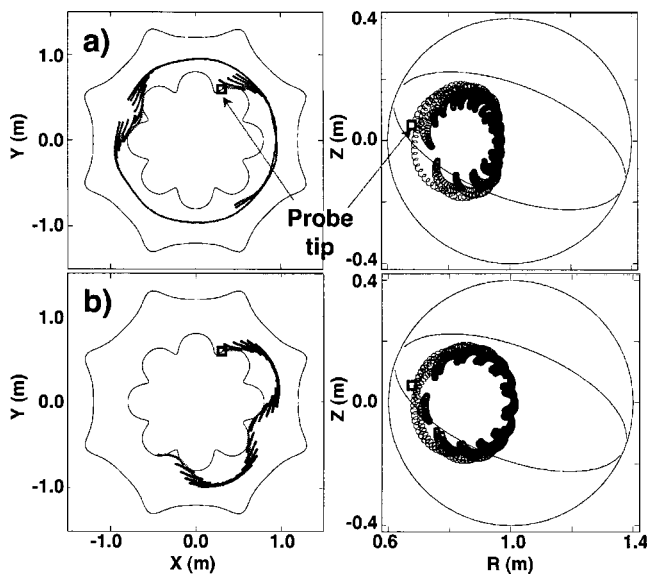


FIG. 4. Orbits of lost helically trapped fast ions. (a) pitch angle $\chi=70^\circ$ at probe position. (b) $\chi=65^\circ$.

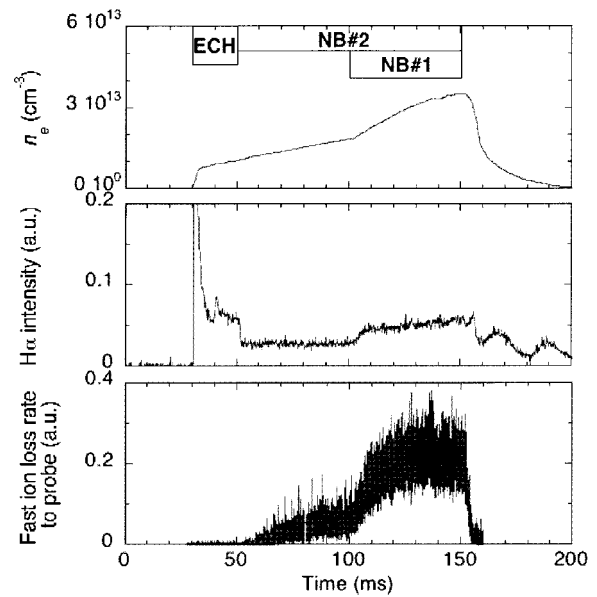


FIG. 5. Fast ion loss rate to probe in $B_t=1.76$ T and $R_{ax}=0.921$ m. Both NBs are tangentially coinjected.

to observe is that the temporal evolution of the scintillation light is different from that of the $H\alpha$ light intensity. No signal is seen in the timing of breakdown due to ECRH although the $H\alpha$ light is very strong in that timing. This means that there is no light leakage into the probe box. When B_t direction is switched from counterclockwise to clockwise, again no signal was observed as expected. This is because ion gyromotion becomes opposite due to reversed B_t direction and then ions cannot strike the scintillator surface. These experimental facts are evidence to support the fact that the measured light originates in escaping fast ions.

IV. SUMMARY

In order to detect unconfined helically trapped fast ions, a new, second escaping fast ion probe has been fabricated and installed for the small R side of the CHS. Because the space available for probe installation is very limited on the small R side, the probe design was carefully performed. In neutral beam heated plasmas, the localized bright light spot appears on the scintillator screen. When B_t is reversed, no signal was observed, suggesting the observed light is due to impact of escaping fast ions onto the scintillator. The analysis indicates that the energy and pitch angle of escaping fast ions we measure are roughly 5–20 keV and 60° – 75° . The orbit calculation shows that detected escaping fast ions have unconfined helically trapped and transitional orbit. These are supposed to be slowed down, pitch angle scattered beam ions. Two escaping fast ion probes are now available in the CHS for the large and small R sides. The fast ion behaviors related to the ripple transport and the MHD-induced transport is going to be investigated in detail by the use of two probes.

ACKNOWLEDGMENTS

The authors wish to express their gratitude to Professor M. Fujiwara and Professor O. Motojima for their continual encouragement. One of the authors (M.I.) wishes to thank Dr. S. Murakami for a fruitful discussion.

¹D. S. Darrow *et al.*, *J. Plasma Fusion Res.* **1**, 362 (1998).

²M. Isobe *et al.*, *Rev. Sci. Instrum.* **70**, 827 (1999).

³D. S. Darrow *et al.*, *Rev. Sci. Instrum.* **70**, 838 (1999).

⁴M. Isobe *et al.*, Proceedings of the 26th European Conference on Con-

trolled Fusion and Plasma Physics, Maastricht (1999), Vol. 23J, p. 21; European Physical Society, CD-ROM (1999).

⁵T. Kondo *et al.*, *Nucl. Fusion* **40**, 1575 (2000).

⁶K. Toi *et al.*, *Nucl. Fusion* **40**, 1349 (2000).

⁷K. Matsuoka *et al.*, in Proceedings of the 12th International Conference on Plasma Physics and Controlled Nuclear Fusion Research, Nice (1988), Vol. 2; IAEA, Vienna (1989), p. 411.

⁸M. Isobe *et al.*, *Nucl. Fusion* **41**, 1273 (2001).

⁹S. J. Zweben, *Nucl. Fusion* **29**, 825 (1989); S. J. Zweben *et al.*, *ibid.* **30**, 1551 (1990).

¹⁰D. S. Darrow *et al.*, *Rev. Sci. Instrum.* **66**, 476 (1995).